Extended Abstracts of the 2004 International Conference on Solid State Devices and Materials, Tokyo, 2004, pp. 732-733

A-9-4

Determination of tunnel mass and thickness of gate oxide including poly-Si/SiO_2 and Si/SiO_2 interfacial transition layers

Hiroshi Watanabe, Daisuke Matsushita and Kouichi Muraoka
Advanced LSI Technology Laboratory, Toshiba Corp., Isogo, Yokohama, 235-8522, Japan
Phone: +81-45-770-3691 Facsimile: +81-45-770-3578 E-mail: pierre.watanabe@toshiba.co.jp

1. Introduction:

Marvelous amount of interests has been recently focused on the interface of MOSFETs having ultra-thin gate oxide, because a drastic change of the band-gap (EG) takes place from the silicon to the oxide [1-4]. Aggressive scaling of MOSFETs enhances effects of the interfacial transition (IFT) layer on CV-JV characteristics. Since the IFT layer makes the interface unclear, it is difficult to determine the oxide thickness (T_{OX}). We include the IFT layers near the interfaces of poly-Si as well as the silicon. We propose the determination method of T_{OX} to overcome this difficulty, and the tunnel mass (m_{OX}) is determined by a self-consistent fitting of CV-JV characteristics with using the T_{OX} and taking into consideration high precise physical models described below [5, 6].

2. Physical models and calculation method:

Firstly, we regard T_{OX} as the distance between the interfaces facing the silicon and the poly-Si and that the IFT layers are included to the gate oxide as shown in Fig. 1. It is further regarded that the IFT layers have a pseudo-alloy structure in which EG linearly changes from the silicon (EG_{Si} of 1.12eV) at the silicon interface to the pure oxide (EG_{OX} of 8.95eV) 4Å away from the interface. An $(Si)_x - (SiO_2)_{1-x}$ structure is assumed inside the IFT layer, and the dielectric constant (K) is then calculated by $K = x \cdot K_{Si} + (1+x) \cdot K_{OX}$ and $x = (EG_{OX}–EG) / (EG_{OX}–EG_{Si})$. Here K_{OX} and K_{Si} are 3.9 for SiO_2 and 11.7 for Si, respectively.

Next, the electron direct tunneling (DT) current is generally a product of the number of tunneling electrons that is determined by the Fermi level (E_F) and the density-of-states (DOS), and the tunneling probability that is determined by m_{OX}, the barrier height (ϕ_B of 3.34eV), the oxide field, and T_{OX} with assuming parabolic E-k dispersion relation. Among them, m_{OX}, ϕ_B and T_{OX} hardly affect the shape of JV characteristics. The m_{OX} is adjusted to perform JV fitting, since T_{OX} is determined by fitting calculated CV characteristics with measured ones obtained by I-V method in parallel mode [7]. On the other hand, E_F, DOS and the oxide field determine the shape of JV characteristics. Since the oxide field is obtained by solving the Poisson equation, all we need is to correctly determine E_F and DOS. The subbands effect revises DOS near the silicon surface since electrons are excluded from energy levels that are lower than the subbands. The weak accumulation layer also revises DOS near the poly-Si surface due to quantum repulsion effect [5], since it excites electrons by the band bending in three-dimensional conduction band. It is more complicated to determine E_F that is mutually interacted with the band-gap narrowing (BGN) and the incomplete ionization of impurities. Since E_F is excluded from the current density equation by the Boltzmann approximation, we have proposed a phenomenological method to self-consistently determine E_F, BGN and the ionization rate in the Fermi-Dirac statistics [6]. Fig. 2 schemes penetrations of the incomplete depletion layer [5] from the poly-Si to the right IFT layer and of the subbands from the silicon to the left IFT layer when gate voltage (V_G) is positive. Fig. 3 schemes penetrations of the weak accumulation layer from the poly-Si to the right IFT layer and of hole-subbands from the silicon to the left IFT layer when V_G is negative. Fig. 4 is a scheme of the present calculation method in which all the physical models and calculation techniques are self-consistently unified in an iterative manner.

Finally, the T_{OX} is re-defined as the average of T_{OX} and the thickness of the pure oxide that does not include the IFT layers.

3. Results:

Considered samples are nMOSFETs with N_A being 1-4E16cm^{-3}, N_D being 8E19-1.4E20cm^{-3} and T_{OX} being 1.4nm-2.8nm, which are determined by the present CV fitting. It is shown in Fig. 5 that when V_G is positive the electrons do not penetrate the left IFT layer from the p-Si whereas the electrons penetrate the right IFT layer from the poly-Si. This is because electrons in lower energy level feel the IFT layers appear narrower, as seen in Fig. 1. It is shown in Fig 6 that when V_G is negative electrons penetrate from the poly-Si to the right IFT layer, whereas the hole-subbands cannot penetrate from the p-Si to the left IFT layer. Therefore, it is found that the IFT layer is more significant near the poly-Si than near the p-Si. Fig. 7 shows the CV-JV fittings, in which (a) a good agreement is obtained in a region including positive and negative gate voltages when the IFT layers are included in both sides of the p-Si and the poly-Si. (b) Neglecting the poly-Si/SiO_2 IFT layer, the calculated JV characteristics become higher than measured ones in the negative V_G region. (c) Neglecting both IFT layers this discrepancy is increased. (d) If K is fixed to K_{OX} inside the IFT layers, then CV-JV characteristics might agree with measurements. The T_{OX} estimated here is however smaller by about 4Å than determined in (a), (b) and (c), as seen in the right figure of Fig. 8. It is further shown in the left figure of Fig 8 that the m_{OX} determined in (a) is within $(0.85\pm0.05) \cdot m_0$ for all samples of T_{OX} ranging from 14 Å to 28Å, where m_0 is the electron rest mass, while the m_{OX} estimated in (d) becomes higher for thinner oxide and it approaches to (a) with the increase of T_{OX}. This is because T_{OX} is underestimated to compensate the decrease of the total K due to K_{OX} inside the IFT layers in the CV fitting. The underestimated T_{OX} increases the DT current, so that the m_{OX} is overestimated in thinner oxide samples to suppress the DT current. In Table I, the estimated m_{OX} is summarized in the cases of (a)-(d). If the JV fitting was performed in the negative V_G region of (b) and (c), then less DT current would be obtained in the positive V_G region, and the m_{OX} would be increased by about 20% for thinner oxide samples, which approaches the result of [8].

4. Conclusions:

The poly-Si/SiO_2 IFT layer is critical to the determination of m_{OX} and T_{OX}. The pseudo-alloy structure assumed in the IFT layers makes T_{OX} close to by ellipsometry within 5% and m_{OX} within $(0.85\pm0.05) \cdot m_0$ with regardless of the T_{OX}, which is clearly advantageous for predicting CV-JV characteristics of near future electron devices with ultra-thin gate insulator.

Acknowledgments:
We are grateful to S. Inumiya, K. Eguchi, and M. Takayanagi for their support in the device fabrication.

References:

[1] D. A. Muller, *et.al*, Nature **399,** 758(1999)
[2] T. Yamasaki, *et.al*. Phys. Rev. **B63**, 115314 (2001)
[3] K. Takahashi, *et.al*. JJAP **41**, 223 (2002)
[4] H. Yang, et.al. IEEE Elec. Dev. Lett. **21**, 76(2000)
[5] H. Watanabe, *et.al*. Ext. abs. SSDM, 270(2003)
[6] H**.** Watanabe and S. Takagi, J. Appl. Phys. **90**, 1600(2001)
[7] H. Suto et al., 748, Ext. abs. SSDM (2002)
[8] Khairurrijal, *et.al.* Appl. Phys. Lett**. 77**, 3580 (2000)

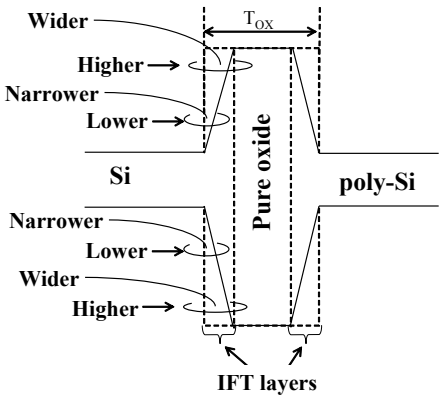

Fig. 1 Present model for IFT layers: these IFT layers are considered both sides.

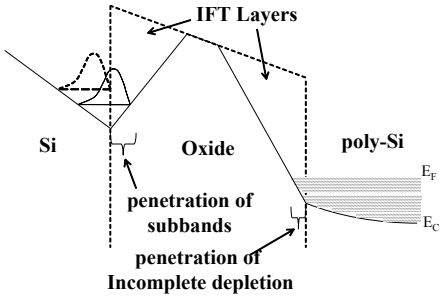

Fig.2 Effects of IFT layers while V_G is positive:

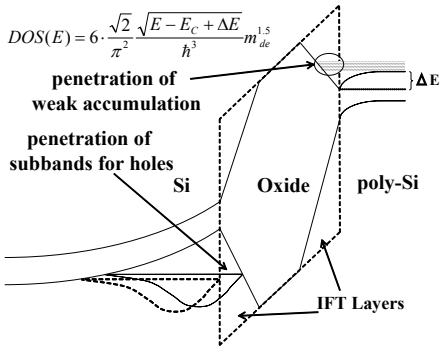

Fig. 3 Effects of IFT layers while V_G is negative:

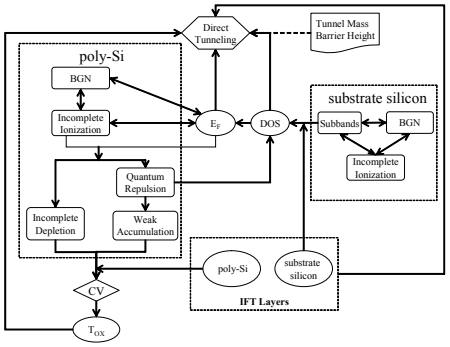

Fig. 4 Scheme of the present calculation and physical models

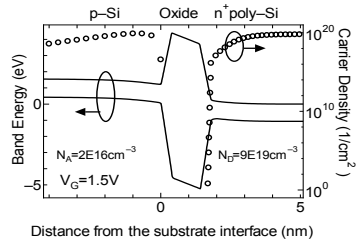

Fig. 5 Calculation result of the electron density profile and the band structure including 4Å IFT layers at both sides when V_G is 1.5V:

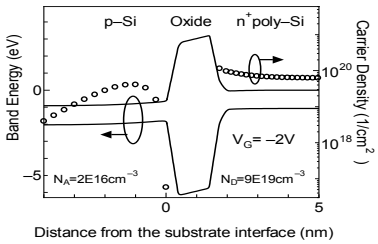

Fig. 6 Calculation results of carrier density profiles and the band structure including 4Å IFT layers at both sides when V_G is –2V:

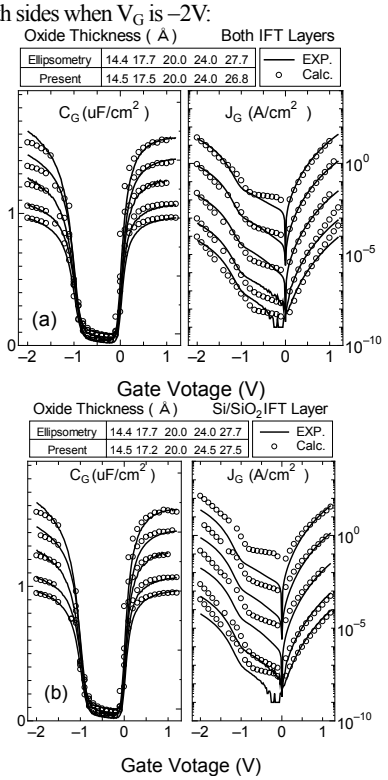

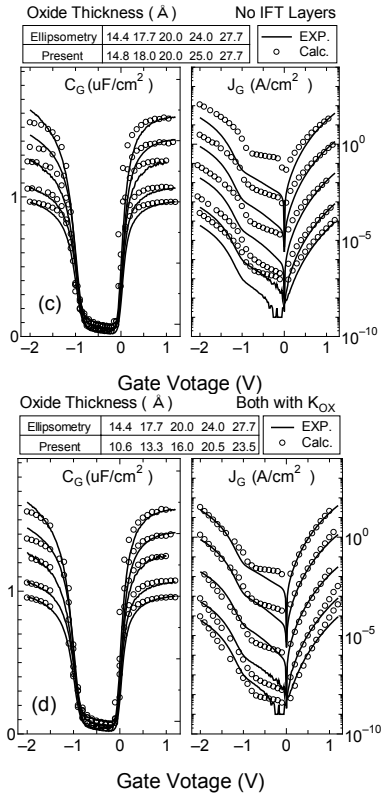

Fig. 7 Agreements of CV-JV characteristics between measurements and calculations: (a) The IFT layers are included in both sides of the p-Si and the poly-Si according to [1]. (b) Only in the side of the p-Si the IFT layer is included according to [4]. (c) From both sides the IFT layers are neglected. (d) The IFT layers in which K is fixed to K_{OX} are included in both sides. The higher data corresponds to thinner oxide.

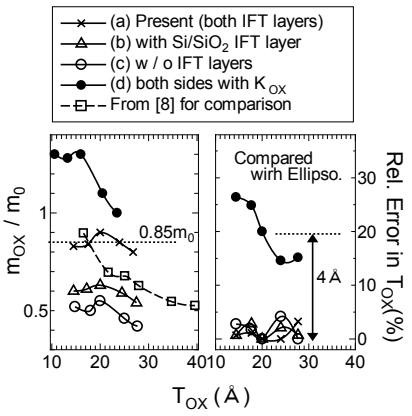

Fig. 8 Tunnel mass and oxide thickness determined in Fig. 7(a)-(d):

Table I Tunnel mass determined in Fig. 7(a)-(d):

	(a)	(b)	(c)	(d)
m_{OX}/m_0	0.85 ±0.05	0.59 ±0.05	0.49 ±0.07	1.15 ±0.15